Weighted Visibility Graph Based WiFi Indoor Positioning Method Using Heuristic Optimization

Turan Göktuğ ALTUNDOĞAN[1*], Mehmet KARAKÖSE[2]

[1] Computer Engineering, Engineering Faculty, Manisa Celal Bayar University, Manisa, Türkiye
[2] Computer Engineering, Engineering Faculty, Firat University, Elazığ, Türkiye
[*1] turan.altundogan@cbu.edu.tr, [2] mkarakose@firat.edu.tr

Abstract: With the widespread use of wireless communication technologies and IoT applications, researchers are developing approaches that utilize WiFi signals for indoor location determination. In this study, indoor positioning process based on heuristic optimization-based methods was performed by creating weighted visibility matrices of access points based on WiFi signal strength (RSSI) values. In the proposed method, the PSO and GA approaches determine the position of the mobile user using a common fitness function based on the visibility weight matrices. The proposed method has been tested on a virtual scenario where position ranges based on RSSI ranges are determined. Both heuristic optimization methods are compared according to different criteria and the positioning process is performed with a maximum error of 3m for the GA based method and a maximum of 1.5m for the PSO based method.

Key words: WiFi Indoor Positioning, Visibility Graphs, PSO, GA.

Sezgisel Optimizasyon Kullanan Ağırlıklı Görünürlük Grafı Tabanlı Kapalı Alan WiFi Konumlandırma Yöntemi

Öz: Kablosuz iletişim teknolojilerinin ve IoT uygulamalarının yaygınlaşmasıyla birlikte araştırmacılar, WiFi sinyallerini iç mekân konum tespiti için kullanan yaklaşımlar geliştirmektedir. Bu çalışmada WiFi sinyal gücü (RSSI) değerlerine dayalı erişim noktalarının ağırlıklı görünürlük matrisleri oluşturularak sezgisel optimizasyon tabanlı yöntemlere dayalı iç mekan konumlandırma işlemi gerçekleştirilmiştir. Önerilen yöntemde, PSO ve GA yaklaşımları, görünürlük ağırlık matrislerine dayalı ortak bir uygunluk fonksiyonu kullanarak mobil kullanıcının konumunu belirler. Önerilen yöntem, RSSI aralıklarına dayalı konum aralıklarının belirlendiği sanal bir senaryo üzerinde test edilmiştir. Her iki sezgisel optimizasyon yöntemi farklı kriterlere göre karşılaştırılmış ve GA tabanlı yöntem için maksimum 3m, PSO tabanlı yöntem için maksimum 1,5m hata ile konumlandırma işlemi gerçekleştirilmiştir.

Anahtar kelimeler: WiFi, Kapalı Alan Konumlandırma, Görünürlük Grafları, PSO, GA.

1. Introduction

Shopping malls, parking garages, airports etc. determination of location information in large indoor areas such as, has become an important need for service users and business managers. Today, indoor positioning systems can be realized with different approaches with the development of wireless communication technologies and the spread of IoT applications. The types of wireless communication used here are generally communication technologies such as WiFi and Bluetooth that every user can carry on their smartphone. WiFi communication technology is communication in the 2.4 – 2.5 GHz or 5.0 GHz frequency range and with the IEEE 802.11 protocol. In WiFi indoor positioning applications, since the distance between the mobile wireless communication source and the communication with the access point can be calculated with a scalar (non-directional) value, there are more than one reference access point in positioning systems. At this point, features such as signal strength (RSSI, Strength) and response time to the signal of wireless communication between access points and mobile users are used.

In the literature, there are many studies focused on indoor positioning [1-14]. In a study, a high-performance positioning process was performed with a method based on the round-trip time (RTT) of WiFi signals [1]. Here, researchers have developed two different position estimation approaches, which they call coarse and fine. The methods proposed in the literature study were tested in an area of 96m^2 with 8 reference access points, and in 80% of the test scenarios, the position determination process was performed below the deviation value of 2.5m.

In another study, the authors investigated the effects of antenna number and antenna connection methods for indoor positioning systems using triangulation [2]. In another study, a comparison of the error depending on the communication frequency was carried out in the WiFi signal strength-based (RSSI) positioning process [3]. In the

---

proposed method, WiFi positioning is performed with a Knn-based method. As a result of the comparison made in the method applied for the 2.4 and 5.0 GHz frequency communications, it was concluded that the location estimation process with the 5.0 GHz communication was more successful. In addition, in the study, the positioning method based on signal strength (RSS) and positioning methods based on path loss were also compared. As a result of this comparison, it was seen that the positioning methods depending on the signal strength gave a higher performance. In another study, an image-based method that automatically configures floor plans for indoor positioning systems (IPS) is proposed [4]. In another study, they developed a classifier in an encoder-decoder structure by using past WiFi signal intensity data for indoor positioning and performed floor and building determination with this classifier [5]. In another study, a method using qr code technology was proposed for IPS [6]. In some studies, Ultra-Wide-Band wireless communication technologies were used [7,8]. With UWB wireless communication technology, indoor positioning can be performed very successfully. So much so that in IPS where WiFi or Bluetooth signals are used, the position error is calculated in the order of meters, while in the UWB-based systems, the error is calculated in the order of centimeters. As a matter of fact, in the study numbered [8], the indoor positioning process was carried out with an error of approximately 9 cm. Despite the high performance of UWB-based methods in positioning applications, they are less preferred in such applications because they have high costs. Table 1 includes the technologies used in studies focused on indoor positioning systems in the literature.

In this study, the visibility weight matrixes depending on the WiFi strength characteristics of the wireless communication of WiFi access points and mobile users are determined and the wireless communication environment is expressed with visibility graphs. Then, the moving position was estimated by heuristic optimization methods using the fitness function based on the visibility weight matrix. Two different methods using GA and PSO heuristic optimizations have been developed to solve the problem. Each method was compared according to calculation speed and performance criteria.

Table 1. Approaches belong to indoor positioning focused studies.

Literature Study	Approach	Motivation
[1]	WiFi	Weighted Scaling
[2]	WiFi	Triangulation
[3]	WiFi	Comparative Study
[4]	Image Processing	Image Processing
[5]	WiFi	Fingerprinting
[6]	QR Code	QR Code Landmark
[7]	UWB	Fingerprinting
[8]	UWB	Range Error Calibration
[9]	WiFi	Fingerprinting
[10]	Bluetooth Beacons	BLE
[11]	WiFi	Triangulation
[12]	WiFi	Temporal – Spatial Fetures
[13]	Bluetooth Beacons	Triangulation
[14]	WiFi	Comparative Study

2. Visibility Graphs

It will be useful to explain the Visibility Graphs in detail for a better understanding of the proposed method. Visibility Graphs, objects, signals, etc. They are graphs in which a weight matrix is used that deals with the visibility relations with each other. Today, visibility graphs are used in many fields such as robotics, signal processing and path planning. In computer science, graphs are expressed as a vector of nodes (V) and a matrix of edges (E). Visibility graphs are also expressed with G=(V, E) as in classical graphs. For a better understanding of the mentioned structure, the visibility matrix of the objects in the environment given in Figure 1 is given in Table 2 and the visibility graph expressed by this matrix is given in Figure 2. As you see, the neighborhoods of objects can see each other in Fig 1, has been assigned 1 and the other neighborhoods has been assigned 0 in weight matrix given in Table 2.
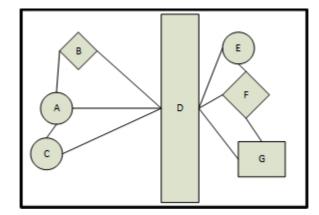
Figure 1. Sample environment belong to given visibility graph in Fig 2.

Table 2. Visibility Matrix Belong To Given Visibility Graph In Fig 2.

	A	B	C	D	E	F	G
A	0	1	1	1	0	0	0
B	1	0	0	1	0	0	0
C	1	0	0	1	0	0	0
D	1	1	1	0	1	1	1
E	0	0	0	1	0	1	0
F	0	0	0	1	1	0	1
G	0	0	0	1	0	1	0

Figure 2. A sample visibility graph.

There are many studies using Visibility Graphs in the literature [15-22]. In one of these, the EEG activities of people with Alzheimer's disease were performed using a visibility graph-based method [15]. The study is a very important example for signal processing applications of Visibility Graphs. Visibility graphs are widely used in signal processing applications today. Especially in neurology, the use of visibility graphs is quite common for the detection of epileptic seizures that occur with the irregularity of EEG signals. In one of the literature studies we discussed, it

focused on the classification of motor images obtained from EEG signals with a versatile, weighted visibility graph and a deep learning-based method [16]. In another study, a method using visibility graphs was used to detect bearing failures in asynchronous motors [17]. In another study, pulse variability-related visibility graphs were used to detect late-onset sepsis in premature infants [18]. In another study, visibility graphs were used to determine the routes of ships [19]. In other studies, methods using visibility graphs are suggested for radar antenna scanning type detection and recognition [20-21]. In another study focused on radars, a visibility graph-based method has been proposed for low probability intercept (LPI) radar signal detection and recognition [22].

In this study, a weighted visibility graph based on the ability of indoor wifi sources to communicate with each other and the RSSI values of wifi signals has been constructed. Reference access points and the visibility of the wifi source to be determined are discussed in the graph. Since the location of the reference points is known, the estimation of the location of the mobile wifi source is performed with two separate methods based on GA and PSO. The proposed methods are tested on a virtual scenario. Existing positioning approaches usually focuses on fingerprinting of WiFi signals broadcasted from different sources. Our motivation in this study is predicting position by constructing a visibility graph using WiFi signals strength and position optimization using heuristic methods. By this way, data collection and tagging which the most difficult step of fingerprinting become unnecessary and this situation makes our method very appliable.

In the virtual scenario, the mobile WiFi source is assumed to be a smartphone, and the WiFi communication distance limit is configured to match the wireless communication capabilities of the smartphones. Since wifi signals are highly susceptible to noise in distance conversions based on RSSI values, value ranges are used. Visibility weights were determined with values between 0-1 assigned to each weight. After testing, the proposed methods were compared according to different criteria.

3. Proposed Approach

In this study, as mentioned before, an indoor positioning method based on Visibility Graphs and heuristic optimization is proposed. The wireless communication technology to be used for positioning here is WiFi. In indoor positioning methods where WiFi communication is used, signal characteristics such as signal strength (RSSI), round-trip time (RTT) belonging to more than one access point and a mobile WiFi source are generally used. In this study, visibility graphs are created based on RSSI values. The weight matrix of the visibility graphs created based on the RSSI values is used in the fitness function in the intuitive optimization step. The general block diagram of the proposed method is given in Figure 3.
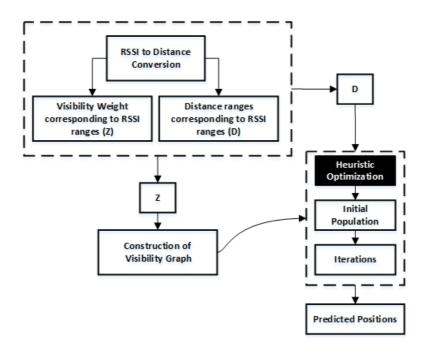

Figure 3. An overall block diagram of Proposed Method.

3.1. RSSI to Distance Conversion and Construction of Visibility Graph

In the proposed method, the aim is to estimate the location of the WiFi source, whose location is desired to be determined, by using the relationship between the RSSI value and the distance to the access point, with a method based on the distances from more than one access point. The mathematical expression used to calculate the RSSI value is given in Equations (1) to (6) [23].

$$P_L(d) = P_L(d_0) + 10nlog(\frac{d}{d_0}) + X_\sigma \tag{1}$$

$$RSSI = P_t - P_L(\text{d}) \tag{2}$$

$$P(d) = P(d_0) - 10nlog\left(\frac{d}{d_0}\right) - X_\sigma \tag{3}$$

$$RSSI = A - 10nlog\left(\frac{d}{d_0}\right) - X_\sigma \tag{4}$$

$$RSSI' = A - 10nlog(d) \tag{5}$$

$$\text{d} = 10^{(A-RSSI)/10n} \tag{6}$$

Here, $P_L(d)$ represents the path loss of the received signal when the distance is d meters. $P_L(d_0)$ refers to the path loss of the reference distance received signal. n denotes the path loss index in a given environment. It shows the speed of path loss increasing with increasing distance. $X\sigma$ s in dB and represents the coverage factor. A represents the signal strength received from the reference point. Here, RSSI' refers to the RSSI values measured multiple times. As can be seen from the equation sets, distance conversion from RSSI can be performed with more than one RSSI value taken from the reference points. But as mentioned before, wifi signals are very sensitive to noise. Therefore, distance ranges corresponding to RSSI value ranges were used while creating visibility graphs. In addition, visibility weights between 0 and 1 are assigned to each value range. In Figure 4, the pseudo-code of the approach introduced for the creation of visibility graphs is given. Here, visibility weights are created according to RSSI intervals. N stands for RSSI intervals, Z stands for visibility weights corresponding to this interval. V represents the wifi resources in the environment and W represents the weight matrix.

3.2. Heuristic Optimization

After the visibility graph was built, two separate methods based on Genetic Algorithm (GA) and Particle Swarm Optimization (PSO) were developed to perform position estimation. In Figure 5, the block diagrams of both methods are given, and in Figure 6, the block diagram that expresses the operations of the individual module used in both methods. As can be seen here, the initial populations for both methods were generated using a random approach. Then, the Euclidean distances of each individual in the population to the reference access points were determined. After this process, the visibility weights corresponding to the distance intervals obtained were determined and the visibility graphs of the individuals were constructed. Here, the fitness function is determined based on the difference averages between the visibility matrices. In both methods, iterations continue until an individual with a fitness value of 1.

```
1. W= zeros(size(v),size(v))
2. for i in size(v):
3. for j in size(v):
4. if(i==j):
5. continue
6. end
7. for k in size(N):
8. if rssi(V[i],V[j]) between N[k]:
9. W[i][j] = Z[k]
10. end
11. end
12. end
13. end
```

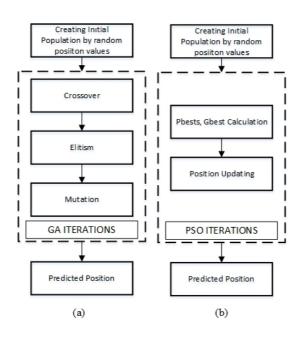**Figure 4.** Obtaining of the weight matrix.

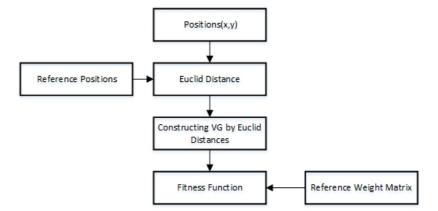**Figure 5.** Heuristic optimization methods.(a:GA,b:PSO)

Figure 6. Processes of individual module using in Heuristic Optimization step.

4. Experimental Results

A virtual scenario was set up to test the proposed method. The first thing to consider here is the maximum distance that the WiFi sources used in the virtual scenario can reach. As it is known, the wifi communications of smart phones have a range of about 30m indoors. However, WiFi communications with an RSSI value below -80 dBm are unstable. Therefore, in the configuration made, a communication scenario with an RSSI value of -80dBm at a distance of 30m was emphasized. RSSI library is integrated into Python programming language for distance and RSSI value conversions. This library provides a function that takes the reference RSSI-distance pair and returns the corresponding RSSI value in meters. At this point, the reference RSSI value we give to the relevant function is -80dBm, and the distance value is 30 meters. In Figure 7, the graph showing the change of the distance value depending on the RSSI value in the relevant configuration is given. In Table 3, the distance ranges and visibility weights corresponding to the selected RSSI intervals are given. As seen in Figure 7, the curve in the graph has a logarithmic character. The reason for this is understood from the mathematical expressions given in Equation 1-6. The proposed method will be tested in a $1800m^2$ virtual area. The area mentioned here has dimensions of 30mx60m. Access points are located at 15m intervals horizontally and vertically.
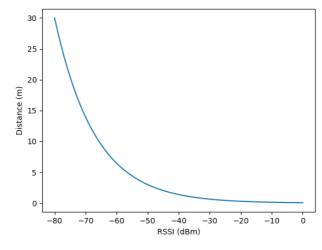
Figure 7. Distance graph based on RSSI.

Table 3. Visibility weights corresponding to rssi and distance range.

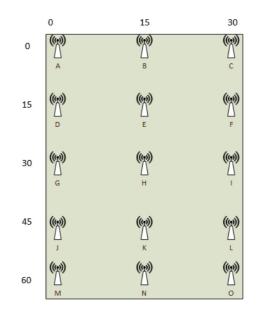| RSSI Range (dBm)	Distance Range (m)	Visibility Weight
<-80	>30	0
-80, -75	30,20	0.2
-75,-70	13,20	0.4
-70,-60	6,13	0.6
-60,-40	1.5,6	0.8
>-40	0,1.5	1.0

Figure 8. Virtual indoor environment.

In Figure 8, a diagram expressing the placement of access points in the virtual environment is given. In Figure 9, the graph expressing the visibility relations of the access points with each other is given.
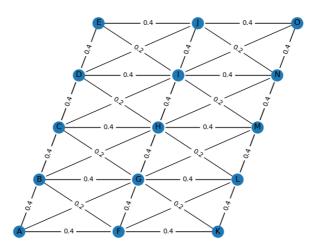
Figure 9. Visibility graph belongs to Access Points.

4.1. Experimental Results of PSO

Users at random positions were added to the virtual environment created for testing the PSO-based positioning method. In Table 4, the randomly added user positions and the predicted positions of these users with PSO, and the Euclidean distance of the predicted position from the actual position are given. The PSO was run at 50 population counts and 150 iterations. In Figure 10, the actual position, and the predicted position of the test case no. In Figure 11, the visibility graph of the test case numbered III is given. In Figure 12, the positions of Test Case V are marked. Figure 13 shows the convergence graph of the PSO.

Table 4. Test results of PSO.

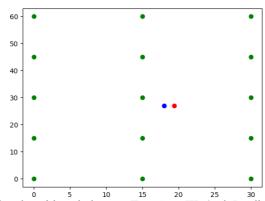| Test No.	Real Position	Predicted Position	Euclid Distance
I	(25,50)	(26,50)	1m
II	(12,20)	(12.43,20.38)	58cm
III	(18,27)	(19.42,26.96)	1.42m
IV	(2,5)	(2.59,5.39)	72cm
V	(7,29)	(7.35,29.07)	36cm

Figure 10. Real and predicted positions belong to Test Case III, (red: Predicted, blue:Real, green:Reference Access points).
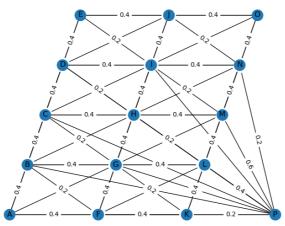
Figure 11. Visibility graph belongs to Test Case III.
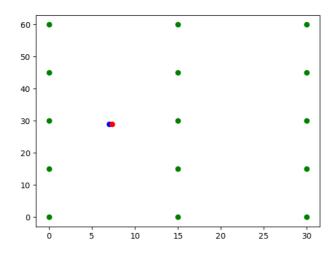

Figure 12. Real and predicted positions belong to Test Case V, (red: Predicted, blue:Real, green:Reference Access points).
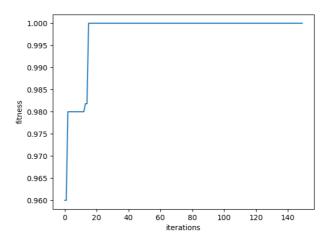

Figure 13. Fitness values belong to iterations.

4.2. Experimental Results of GA

Users at random positions were added to the virtual environment created for testing the GA-based positioning method. In Table 5, randomly added user positions and their predicted positions with PSO, and the Euclidean distance of the predicted position from the actual position are given. The GA was run for 10 populations and 1500 iterations. In Figure 14, the actual position and the predicted position of the test case IV on the virtual environment are marked. In Figure 15, the visibility graph of the test case no. III is given. In Figure 16, the positions of Test Case V are marked. Figure 17 shows the convergence graph of the GA.

Table 5. Test results of GA.

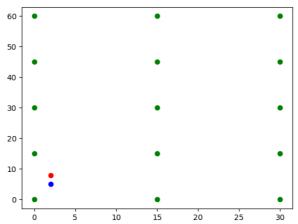| Test No.	Real Position	Predicted Position	Euclid Distance
I	(25,50)	(25,49)	1m
II	(12,20)	(11,19)	1.41cm
III	(18,27)	(18,26)	1m
IV	(2,5)	(2,8)	3m
V	(7,29)	(7,28)	1m

Figure 14. Real and predicted positions belong to Test Case IV, (red: Predicted, blue:Real, green:Reference Access points).

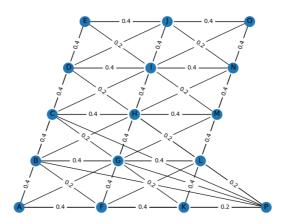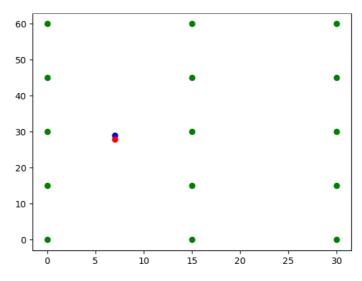**Figure 15.** Visibility graph belongs to Test Case IV.

142

Figure 16. Real and predicted positions belong to Test Case V, (red: Predicted, blue:Real, green:Reference Access points).
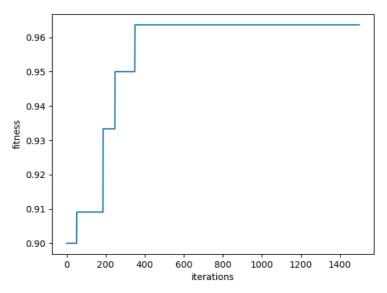

Figure 17. Fitness values belong to iterations.

5. Discussion

When the experimental results are examined, it's seen that our position estimation approaches has achieved with a meter degree error. The results of comparisons between PSO and GA based methods proofed that the PSO based methods performance is better than GA based method. Because, almost all test error of PSO based approach is in centimeter degree, only one test error of GA based approach in centimeter degree. Besides, when Figures 13 and 17 are compared, PSO based method converges the optimum results faster than GA based method. Figure 10 and Figure 12 indicate us the real position and predicted positions and sensibility of both methods.

6. Conclusions

In this study, visibility graphs depending on Wi-Fi signal strength were created for indoor positioning and these graphs were used in the fitness function of two different heuristics for position estimation. When the experimental results are examined, it is seen that the PSO-based position estimation method works with a higher performance than the GA-based position estimation method. This situation is thought to be due to the presence of the position update approach in the working principle of the PSO and the search in the solution space with the crossover approach in GA. In addition, GA gave the results without converging the fitness value to 1.0 in many estimation

143

processes, PSO gave the results by obtaining a fitness value of 1.0 in each study. If we consider the working speed of the methods as another comparison criterion, it has been observed that PSO has a great advantage over GA (almost 250 times). In general, the developed approaches have achieved very efficient results in terms of performance (error < 1.5m) and position estimation time (340 ms) for PSO.

References

[1] Yan S, Luo H, Zhao F, Shao W, Li Z and Crivello A, "Wi-Fi RTT based indoor positioning with dynamic weighted multidimensional scaling," 2019 International Conference on Indoor Positioning and Indoor Navigation (IPIN), 2019, pp. 1-8, doi: 10.1109/IPIN.2019.8911783.

[2] Yuan D et al., "Model Checking Indoor Positioning System With Triangulation Positioning Technology," 2018 9th International Conference on Information Technology in Medicine and Education (ITME), 2018, pp. 862-866, doi: 10.1109/ITME.2018.00193.

[3] Maung NAM, and Zaw W, "Comparative Study of RSS-based Indoor Positioning Techniques on Two Different Wi-Fi Frequency Bands," 2020 17th International Conference on Electrical Engineering/Electronics, Computer, Telecommunications and Information Technology (ECTI-CON), 2020, pp. 185-188, doi: 10.1109/ECTI-CON49241.2020.9158211.

[4] Jaworski W, Wilk P, Juszczak M, Wysoczańska M and Lee AY, "Towards automatic configuration of floorplans for Indoor Positioning System," 2019 International Conference on Indoor Positioning and Indoor Navigation (IPIN), 2019, pp. 1-7, doi: 10.1109/IPIN.2019.8911747.

[5] Joseph R and Sasi SB, "Indoor Positioning Using WiFi Fingerprint," 2018 International Conference on Circuits and Systems in Digital Enterprise Technology (ICCSDET), 2018, pp. 1-3, doi: 10.1109/ICCSDET.2018.8821184.

[6] Li Z and Huang J, "Study on the use of Q-R codes as landmarks for indoor positioning: Preliminary results," 2018 IEEE/ION Position, Location and Navigation Symposium (PLANS), 2018, pp. 1270-1276, doi: 10.1109/PLANS.2018.8373516.

[7] Blazek J, Jiranek J and Bajer J, "Indoor Passive Positioning Technique using Ultra Wide Band Modules," 2019 International Conference on Military Technologies (ICMT), 2019, pp. 1-5, doi: 10.1109/MILTECHS.2019.8870099.

[8] Perakis H and Gikas V, "Evaluation of Range Error Calibration Models for Indoor UWB Positioning Applications," 2018 International Conference on Indoor Positioning and Indoor Navigation (IPIN), 2018, pp. 206-212, doi: 10.1109/IPIN.2018.8533755.

[9] Molina B, Olivares E, Palau CE and Esteve M, "A Multimodal Fingerprint-Based Indoor Positioning System for Airports," in IEEE Access, vol. 6, pp. 10092-10106, 2018, doi: 10.1109/ACCESS.2018.2798918.

[10] Andrushchak V, Maksymyuk T, Klymash M and Ageyev D, "Development of the iBeacon's Positioning Algorithm for Indoor Scenarios," 2018 International Scientific-Practical Conference Problems of Infocommunications. Science and Technology (PIC S&T), 2018, pp. 741-744, doi: 10.1109/INFOCOMMST.2018.8632075.

[11] Teoman E and Ovatman T, "Trilateration in Indoor Positioning with an Uncertain Reference Point," 2019 IEEE 16th International Conference on Networking, Sensing and Control (ICNSC), 2019, pp. 397-402, doi: 10.1109/ICNSC.2019.8743240.

[12] Shao W, Luo H, Zhao F, Tian H, Yan S and Crivello A, "Accurate Indoor Positioning Using Temporal–Spatial Constraints Based on Wi-Fi Fine Time Measurements," in IEEE Internet of Things Journal, vol. 7, no. 11, pp. 11006-11019, Nov. 2020, doi: 10.1109/JIOT.2020.2992069.

[13] Pakanon N, Chamchoy M and Supanakoon P, "Study on Accuracy of Trilateration Method for Indoor Positioning with BLE Beacons," 2020 6th International Conference on Engineering, Applied Sciences and Technology (ICEAST), 2020, pp. 1-4, doi: 10.1109/ICEAST50382.2020.9165464.

[14] Ang JLF, Lee WK and Ooi BY, "GreyZone: A Novel Method for Measuring and Comparing Various Indoor Positioning Systems," 2019 International Conference on Green and Human Information Technology (ICGHIT), 2019, pp. 30-35, doi: 10.1109/ICGHIT.2019.00014.

[15] Cai L, Deng B, Wei X, Wang R and Wang J, "Analysis of Spontaneous EEG Activity in Alzheimer's Disease Using Weighted Visibility Graph," 2018 40th Annual International Conference of the IEEE Engineering in Medicine and Biology Society (EMBC), 2018, pp. 3100-3103, doi: 10.1109/EMBC.2018.8513010.

[16] Samanta K, Chatterjee S and Bose R, "Cross-Subject Motor Imagery Tasks EEG Signal Classification Employing Multiplex Weighted Visibility Graph and Deep Feature Extraction," in IEEE Sensors Letters, vol. 4, no. 1, pp. 1-4, Jan. 2020, Art no. 7000104, doi: 10.1109/LSENS.2019.2960279

[17] Roy SS, Chatterjee S, Barman R, Roy S and Dey S, "Bearing Fault Detection in Induction Motors Employing Difference Visibility Graph," 2020 IEEE International Conference on Power Electronics, Drives and Energy Systems (PEDES), 2020, pp. 1-4, doi: 10.1109/PEDES49360.2020.9379635.

[18] León C, Carrault G, Pladys P and Beuchée A, "Early Detection of Late Onset Sepsis in Premature Infants Using Visibility Graph Analysis of Heart Rate Variability," in IEEE Journal of Biomedical and Health Informatics, vol. 25, no. 4, pp. 1006-1017, April 2021, doi: 10.1109/JBHI.2020.3021662.

[19] Kulbiej E, "Autonomous Vessels' Pathfinding Using Visibility Graph," 2018 Baltic Geodetic Congress (BGC Geomatics), 2018, pp. 107-111, doi: 10.1109/BGC-Geomatics.2018.00026.

[20] Songtao L, Zhenshuo L, Yang G and Zhenming W, "Automatic radar antenna scan type recognition based onlimited penetrable visibility graph," in Journal of Systems Engineering and Electronics, vol. 32, no. 2, pp. 437-446, April 2021, doi: 10.23919/JSEE.2021.000037.

[21] Wan T, Fu X, Jiang K, Zhao Y and Tang B, "Radar Antenna Scan Pattern Intelligent Recognition Using Visibility Graph," in IEEE Access, vol. 7, pp. 175628-175641, 2019, doi: 10.1109/ACCESS.2019.2957769.

[22] Tao W, J. Kaili, Jingyi L, Yanli T and Bin T, "Detection and recognition of LPI radar signals using visibility graphs," in Journal of Systems Engineering and Electronics, vol. 31, no. 6, pp. 1186-1192, Dec. 2020, doi: 10.23919/JSEE.2020.000091.

[23] Shang F, Su W, Wang Q, Gao, H and Fu Q. "A location estimation algorithm based on RSSI vector similarity degree" *International Journal of Distributed Sensor Networks*, *10*(8), 2014, 371350.